MOLECULAR AND CELLULAR BIOLOGY, Apr. 1997, p. 2020–2029 Vol. 17, No. 4
0270-7306/97/$04.00+0
Copyright © 1997, American Society for Microbiology

Fragments of ATM Which Have Dominant-Negative or Complementing Activity

SUSAN E. MORGAN,[1] CHRISTINE LOVLY,[1] TEJ K. PANDITA,[2] YOSEF SHILOH,[3] AND MICHAEL B. KASTAN[1]*

The Johns Hopkins Oncology Center, Baltimore, Maryland 21205[1]; Center for Radiological Research, Columbia University, College of Physicians and Surgeons, New York, New York 10032[2]; and Department of Human Genetics, Sackler School of Medicine, Tel Aviv University, Ramat Aviv 69978, Israel[3]

Received 10 December 1996/Returned for modification 23 January 1997/Accepted 27 January 1997

The ATM protein has been implicated in pathways controlling cell cycle checkpoints, radiosensitivity, genetic instability, and aging. Expression of ATM fragments containing a leucine zipper motif in a human tumor cell line abrogated the S-phase checkpoint after ionizing irradiation and enhanced radiosensitivity and chromosomal breakage. These fragments did not abrogate irradiation-induced G_1 or G_2 checkpoints, suggesting that cell cycle checkpoint defects alone cannot account for chromosomal instability in ataxia telangiectasia (AT) cells. Expression of the carboxy-terminal portion of ATM, which contains the PI-3 kinase domain, complemented radiosensitivity and the S-phase checkpoint and reduced chromosomal breakage after irradiation in AT cells. These observations suggest that ATM function is dependent on interactions with itself or other proteins through the leucine zipper region and that the PI-3 kinase domain contains much of the significant activity of ATM.

Ataxia telangiectasia (AT) is a rare human autosomal recessive disorder with a wide variety of phenotypic manifestations. AT patients exhibit progressive cerebellar ataxia with degeneration of Purkinje cells, oculocutaneous telangiectases, hypersensitivity to ionizing radiation (IR) and radiomimetic drugs, thymic hypoplasia with variable cellular and humoral immune dysfunction, hypogonadism, growth retardation, and premature aging (20, 55). AT homozygotes have an approximately fivefold increased risk of developing leukemia or lymphoblastic lymphomas and usually die by the second or third decade of life (22, 59). Epidemiologic studies have suggested that AT heterozygotes (approximately 1% of the population) may be at a three- to fivefold increased risk of developing cancer (58, 59), although this has not yet been confirmed by population-based studies of AT carriers.

Cells derived from AT patients, such as fibroblasts and lymphoblasts, exhibit a variety of abnormalities in culture such as cytoskeletal defects, hypersensitivity to IR, higher requirements for serum growth factors, and a reduced life span in culture (12, 36, 42). AT cells have elevated frequencies of spontaneous and induced chromosomal aberrations, including defects in immune gene rearrangements and abnormally high spontaneous rates of intrachromosomal recombinations (30, 34, 37, 44, 47). AT cells also appear to have suboptimal G_1, S, and G_2 cell cycle checkpoints induced by DNA damage. The lack of an S-phase checkpoint in AT cells was noted by Painter and colleagues as the continued synthesis of DNA in AT cells at early time points following irradiation (known as radioresistant DNA synthesis [RDS]) (26, 43). Abnormalities in the irradiation-induced G_1 checkpoint response are manifested as suboptimal induction of p53 protein and the p53-dependent gene products, $p21^{WAF1/cip1}$, mdm2, and gadd45, after IR of AT cells (6, 27, 29, 31). A defective G_2 checkpoint is evident when AT cells irradiated in G_2 continue to progress into mitosis while normal cells arrest in G_2 (3).

The gene responsible for AT was recently identified by positional cloning and was designated *ATM* (for AT mutated) (53, 54). The *ATM* gene is approximately 150 kb in length and encodes a 13-kb mRNA transcript that is expressed in a wide variety of tissues. The open reading frame (ORF) of the *ATM* transcript encodes a protein of 3,056 amino acids with a predicted molecular mass of 350 kDa (53, 54). ATM belongs to an expanding family of large eukaryotic proteins involved in cell cycle control and DNA repair and recombination. This family of proteins has been grouped together with ATM primarily due to the homology of their carboxy termini to the 100-kDa catalytic subunit of the mammalian signal transduction mediator, phosphatidylinositol 3-kinase (PI-3 kinase).

PI-3 kinases have been widely studied and appear to participate in many cellular processes including insulin-dependent glucose transport, growth factor responses, and cellular differentiation (9, 11, 18, 25, 61). Members of this family include the yeast TOR1 and TOR2 proteins as well as the mouse and human homologs mTOR (RAFT1) and FRAP, respectively, all of which are involved in the G_1/S cell cycle progression (4, 23, 24, 32, 49, 50, 56). Other members of this family include the yeast Tel1p protein, which is involved in telomere length maintenance (17, 41), and the yeast and *Drosophila* cell cycle checkpoint-DNA recombination and repair proteins, Mec1p (Esr1/Sad3) (2, 28, 63), Rad3 (1, 10), and Mei-41 (19). In addition, DNA-dependent protein kinase (DNA-PK) is a family member which has documented serine/threonine protein kinase activity. DNA-PK is activated by DNA double-strand breaks and is suggested to play a role in DNA damage detection and/or DNA repair and V(D)J recombination (15, 21, 60, 62). The similarities between ATM and this family of PI-3 kinase-like proteins suggest involvement of ATM in signal transduction, cellular responses to DNA damage, and cell cycle control. The observation that the PI-3 kinase domain is affected by either truncation or point mutations in virtually all AT patients sug-

* Corresponding author. Mailing address: The Johns Hopkins Oncology Center, Ross Bldg., Rm. 345, 720 Rutland Ave., Baltimore, MD 21205. Phone: (410) 614-2747. Fax: (410) 614-4095. E-mail: mbkastan@welchlink.welch.jhu.edu.

gests that this catalytic domain may play an essential role in ATM function (5, 14).

One possible approach to investigating cell-type-specific effects of ATM dysfunction in physiological processes such as growth factor responses, cell cycle control, radiosensitivity, or apoptosis is to generate a variety of different cell types with altered ATM function. We have attempted to accomplish this by generating dominant-negative fragments of the ATM protein which can be expressed in cell lines and inhibit ATM function. ATM fragments containing the putative leucine zipper (LZ) motif were chosen for these studies since proteins containing LZ regions typically form homo- or heterodimers. Overexpression of such truncated proteins has previously been shown to result in dominant-negative inhibition of protein function (8, 16). We demonstrate that expression of ATM protein fragments containing the LZ motif in a human tumor cell line resulted in a dominant-negative inhibition of ATM function as revealed by decreased clonogenic survival after irradiation, enhanced chromosomal instability following irradiation, and development of RDS.

The role of the PI-3 kinase domain of ATM was also investigated by generating and expressing a PI-3 kinase-containing ATM protein fragment in simian virus 40 (SV40)-transformed AT fibroblasts and assessing the ability of this truncated protein to complement the AT phenotype. Expression of the PI-3 kinase domain in AT cells resulted in the restoration of the irradiation-induced S-phase arrest, enhanced clonogenic survival, and reduced chromosomal breakage after irradiation. This suggests that many of the functions of ATM may reside in this catalytic domain. Taken together, these studies provide a novel means by which ATM protein function can be manipulated and characterized, such that cell-type-specific signalling pathways involving ATM can be addressed.

MATERIALS AND METHODS

Cell culture and irradiation treatment. Epstein-Barr virus (EBV)-immortalized lymphoblastoid cell lines from normal individuals (GM2184) and AT homozygotes (GM1526) were cultured in RPMI-1640 supplemented with 15% fetal calf serum (FCS). SV40-transformed fibroblast cell lines from normal individuals (GM637) and AT homozygotes (GM5849) were cultured in Dulbecco's modified eagle medium (DMEM) supplemented with 15% FCS. All cell lines were obtained from the Human Genetic Mutant Cell Repository (Camden, N.J.). The RKO colorectal carcinoma cell line (31) and the retroviral packaging cell line PA317 (American Type Culture Collection [ATCC], Rockville, Md.) were maintained in DMEM with 10% FCS. All cell lines were grown at 37°C in a humidified 5% CO_2 atmosphere. Cells were irradiated with a ^{137}Cs source at a dose rate of approximately 100 rad/min.

Generation and expression of *ATM* cDNA fragments in a retroviral packaging cell line. Three human *ATM* cDNA fragments (ENA/FB2F, FB2F, and PI3K) were PCR amplified with *ATM* cDNA clones as templates. These constructs were generated by using the following reaction conditions. FB2F and PI3K *ATM* cDNA templates (1 μg) were added to a 100-μl total volume containing 1× PCR buffer (10 mM Tris-HCl [pH 8.3], 50 mM KCl, 2.5 mM $MgCl_2$, 0.01% gelatin) and 200 μM (each) dCTP, dATP, dGTP, and dTTP. To the mixture were added 50 pmol each of two synthetic oligonucleotides. Pfu DNA polymerase (2.5 U; Stratagene) was added to the PCR mixture, and DNA amplification was performed for 20 cycles in a DNA thermal cycler (MJ Research, Inc.; denaturation at 95°C for 45 s, annealing at 50°C for 1 min, and extension at 72°C for 4 min for each cycle). After amplification, 10 μl of each PCR mixture was fractionated by electrophoresis to confirm the size of the amplification products. A 1.4-kb FB2F cDNA fragment was amplified with the forward primer 5′-CGTGGGATCCGC CATG AATGACATTGCAGAT-3′ (*ATM* ORF nucleotides [nt] 2433 to 2451), which contains a Kozak consensus translation initiation sequence and a *Bam*HI restriction site, and the reverse primer 5′-ACGCGTCGACTCAGTA GTTTA ATAAAATAAAAGG-3′ (*ATM* ORF nt 3703 to 3724), which contains a *Sal*I restriction site. A 1.2-kb PI3K cDNA fragment was amplified with the forward primer 5′-GATGAATTCGCCACCA TGGAAATTAAGGTGGACC-3′ (*ATM* ORF nt 7998 to 8017 nt), which contains a Kozak consensus sequence and an *Eco*RI restriction site, and the reverse primer 5′-ACCGCTCGAGTACT GAA GATCACACCCAAG-3′ (*ATM* ORF nt 9199 to 9179), which contains a *Xho*I restriction site.

The ENA/FB2F *ATM* cDNA was generated by using the PCR overlap extension technique. PCR amplification of each half of the ENA/FB2F cDNA was performed separately, followed by joining of the halves in a third PCR. The ENA cDNA half was generated with the forward primer 5′-CGTGGGATCCACCA TGAGTCTAGTACTT-3′ (leucine 1) (*ATM* ORF nt 1 to 15), which contains a *Bam*HI restriction site, and the reverse primer 5′-ATGGATGACTG ATCCTC CAC-3′ (leucine 2) (*ATM* ORF nt 2545 to 2565). The FB2F cDNA half was generated with the forward primer 5′-GTGGAGGATCAGTCATCCAT-3′ (leucine 3) (*ATM* ORF nt 2545 to 2565) and the reverse primer 5′-ACGCGTC GACTCAGTAGTTT AATAAAATAAAAGG-3′ (leucine 4) (*ATM* ORF nt 3703 to 3724), which contains a *Sal*I restriction site. Primer leucine 2 contains at its 5′ end 20 nt complementary to the leucine 3 primer. Conditions for PCR amplification were as described above. The two separate PCR-amplified DNA fragments containing the overlapping, complementary sequences were gel purified (β-agarase, N.E. Biolabs), mixed together (1 μg each), and subjected to a second PCR amplification with a pair of external oligonucleotides, leucine 1 and leucine 4. Following amplification the sizes of the products were confirmed by agarose gel electrophoresis. The two sets of primers, leucine 1-leucine 2 and leucine 3-leucine 4, constructed a 3.6-kb cDNA fragment which encodes the ENA/FB2F protein.

The PCR-generated *ATM* products (10 μg) and the retroviral expression vectors pBABE and LXSN (20 μg; obtained from Alan Friedman, Johns Hopkins Oncology Center) (39, 40) were digested sequentially with the appropriate restriction endonucleases (5 U/μg, 37°C, 3 h). Digestion products were fractionated by electrophoresis and gel purified, and the *ATM* cDNA fragments were ligated separately into a similarly cleaved pBABE or LXSN retroviral expression vector. Following ligation, competent DH5-α *Escherichia coli* cells (Gibco BRL) were transformed with one-tenth of the ligation reaction. Ampicillin-resistant bacterial colonies resulting from the transformation were randomly chosen and used for plasmid DNA isolation (Wizard Minipreps DNA purification system; Promega Madison, Wis.). The identities of the subcloned *ATM* cDNAs were confirmed by plasmid DNA digestion and DNA sequencing (51).

The pBABE-FB2F, pBABE-ENA/FB2F, LXSN-PI3K, and vector-alone DNA constructs were introduced into the amphotropic packaging cell line PA317 (ATCC) by $CaPO_4$-mediated transfection (5). Forty-eight hours posttransfection, the PA317 cells transfected with pBABE-LZ constructs were placed in puromycin selection medium (4 μg/ml, final concentration) while the PA317 cells transfected with the LXSN-PI3K constructs were placed in neomycin selection medium (800 μg/ml, final concentration). After drug-resistant colony formation (7 to 14 days of selection), polyclonal pools were tested for the production of a high viral titer by using NIH 3T3 fibroblasts as a target cell line.

Generation of *ATM* fragment-expressing clonal populations. Infectious supernatant from these stable pBABE-LZ or LXSN-PI3K retrovirus-producing PA317 cell lines was used to infect the RKO colorectal carcinoma cell line, normal GM637 or AT GM5849 SV40-transformed fibroblasts as described by Miller et al. (39). Fresh viral supernatant derived from logarithmically growing transfected PA317 cells was mixed with Polybrene (2 μg/ml, final concentration) and used to infect the target cells (4 h, 37°C) for 3 consecutive days. Forty-eight hours following the last viral infection, the cells were placed in selection medium. After drug-resistant colony formation (7 to 14 days), monoclonal populations containing FB2F, ENA/FB2F, PI3K, or vector-alone constructs were isolated.

RT-PCR analysis. Total RNA was extracted from parental and infected monoclonal cell lines (Trizol reagent; Gibco BRL) and used as substrate for reverse transcription (RT)-PCR according to the manufacturer's instructions (Gibco BRL). Briefly, 5 μg of total RNA was reverse transcribed in a 20-μl reaction mixture containing 5 pmol of an oligonucleotide primer complementary to the 3′ end of the transcribed strand of either the retroviral SV40 promoter sequence (5′-GGGACTATGGTTGCTGAC TAATTG-3′), the FB2F *ATM* cDNA sequence (*ATM* ORF 3703 to 3724 nt, described above), or the PI3K *ATM* cDNA sequence (*ATM* ORF 9179 to 9199 nt, described above) and 50 mM Tris (pH 8.3), 75 mM KCl, 15 mM $MgCl_2$, 0.1 mM dithiothreitol, 0.5 mM each deoxynucleoside triphosphate, and 200 U of Superscript RT. The reaction was incubated at 42°C for 50 min, terminated at 70°C for 15 min, and then incubated with RNaseH (10 U, 37°C, 20 min). The cDNA products derived from the RT reactions were used as templates (2 μl of the RT mixture) for PCR amplification with the appropriate primer pairs and conditions as described above. After amplification, 10 μl of each reaction mixture was fractionated by agarose gel electrophoresis to confirm the size of the RT-PCR products.

RDS analysis. Inhibition of DNA synthesis following IR was assessed by a method similar to that described by Painter and Young (43). Briefly, logarithmically growing cells (5×10^4 cells per dish) were incubated with DMEM containing 10 nCi of [^{14}C]thymidine per ml (specific activity, 50 mCi/mmol) for approximately 48 h to control for total DNA content between samples. The medium was replaced with nonradioactive DMEM and incubated for 24 h, and the cells were then treated with 0 or 4 Gy of IR, incubated at 37°C for 30 min, and then pulse-labeled (15 min) with 2.5 μCi/ml of [^3H]thymidine. The cells were harvested, washed twice with phosphate-buffered saline (PBS; pH 7.4), and fixed in 70% methanol. The cell suspension was filtered through GF/C (Whatman) filters, which were rinsed sequentially with 70 and 95% methanol, air dried, and assayed for radioactivity in a liquid scintillation counter. The resulting ratios of $^3H/^{14}C$, corrected for channel crossover of the isotopes, were measures of DNA synthesis activity.

Immunoblots. Cells were harvested, counted, and solubilized in Laemmli sample buffer for immunoblot analysis as previously described (6). Thirty micro-

grams of protein lysate was loaded into each lane, and equal loading was confirmed by fast green staining of the membrane. Immunoblots for p53 and p21 proteins were done with anti-p53 antibody Ab-6 (diluted 1:500 in blocking solution; Oncogene Science, Uniondale, N.Y.) or anti-p21 antibody (diluted 1:300 in blocking solution; Pharmingen, San Diego, Calif.).

Assay for G_2 checkpoint and chromosomal gaps and breaks. The G_2 cell cycle checkpoint and chromosomal aberrations in mitosis were assessed by evaluating the number of metaphase chromosome spreads or the number of breaks and gaps per metaphase in logarithmically growing cell lines following exposure to 0 or 1 Gy of IR. Following treatment with 0 or 1 Gy of IR, cells were incubated at 37°C and treated with colcemid (0.1 μg/ml; Gibco BRL) for 30 to 60 min prior to each cell harvest. Cells were harvested at either 30, 90, or 150 min after IR (2,800 × *g*, 10 min, 4°C). Cell pellets were washed with PBS, incubated in Zenon's hypotonic buffer (40 mM KCl, 20 mM HEPES, 0.5 mM EGTA, pH 7.4) for 20 min at 37°C, and fixed in a 3:1 ratio of methanol to acetic acid. Slides were made and stained by using standard conditions (13).

Clonogenic assays. Cell lines were plated in triplicate at limiting dilutions into 6-well plates, incubated for 17 h, and then exposed to a range of doses of IR (0 to 6 Gy) followed by incubation for 1 to 2 weeks at 37°C. Prior to counting colonies, the culture medium was decanted from each well, and the cells were fixed in 95% methanol and stained with crystal violet. The mean colony counts ± standard errors (SE) appear in the figures.

Chromosome studies. (i) Interphase chromosomes. Premature chromosome condensation was used to visualize interphase chromosome damage immediately after irradiation in G_1-phase cells. Plateau-phase cells were placed on ice for 20 min before irradiation, irradiated with ^{137}Cs γ-irradiator at the dose rate of 1.0 Gy/min, trypsinized, and fused with the mitotic HeLa cells. Detailed procedures for HeLa cell accumulation, cell fusion, chromosome preparation, differential staining, and chromosome breakage analysis have been previously described (46).

(ii) Metaphase chromosomes. Plateau-phase cells were irradiated as described above, incubated for 24 h postirradiation, and then trypsinized and plated. Metaphase chromosomes were prepared by a procedure described earlier (45). Giemsa-stained metaphase chromosomes were analyzed for chromosomal aberrations from first cycle metaphases only.

RESULTS

Construction and expression of *ATM* cDNA fragments. *ATM* fragments containing either the LZ motif (FB2F), the LZ motif along with the entire 5′ *ATM* coding region (ENA/FB2F), or the carboxy-terminal PI-3 kinase domain (Fig. 1A) were generated by PCR. Each gel-purified, PCR-generated cDNA, after sequential restriction enzyme digestion, was subcloned into either the LXSN or pBABE retroviral expression vector. Expression of the *ATM* cDNA fragments is under control of the long terminal repeat promoter, while expression of the puromycin gene is under the control of the SV40 promoter (Fig. 1B). Sequencing of the *ATM* cDNAs confirmed that no PCR-induced mutations were generated in any of these fragments.

RKO colorectal tumor cells were infected with either recombinant control pBABE, pBABE-FB2F, or pBABE-ENAFB2F retroviruses by a method described by Miller et al. (39). Puromycin-resistant clones were isolated and screened for the expression of the desired *ATM* cDNA fragment by RT-PCR. To differentiate between the expression of endogenous *ATM* and recombinant pBABE-*ATM* fragments, an oligonucleotide primer was used in the RT reaction which is complementary only to the pBABE-SV40 vector sequence (Fig. 1B, primer 1). The use of primer 1 in the RT-PCR resulted in the selective amplification of pBABE-FB2F or -ENA/FB2F cDNAs but not of endogenous *ATM* sequences. To detect endogenous *ATM* expression in the parental RKO cell line, an oligonucleotide primer was used in a RT reaction which is complementary to the 3′ end of the transcribed strand of the *ATM* FB2F RNA sequence (Fig. 1B, primer 3).

The cDNA products derived from the RT reactions were used as templates for PCR amplification. RT-PCR resulted in amplifications of approximately 1.5-kb or 1.4-kb cDNA products in pBABE-FB2F clones 3 and 12 (Fig. 1C, lanes h and i and lanes k and l). The size of the 1.4-kb product was in agreement with the amplified FB2F plasmid DNA and the amplified, endogenous *ATM* FB2F cDNA (Fig. 1C, lanes a and b, respectively). RT-PCR of pBABE-ENA/FB2F clone 18 resulted in amplification of an approximately 3.7-kb cDNA product (Fig. 1C, lane n). The size of this product was similar to the PCR-amplified ENA/FB2F plasmid DNA (Fig. 1C, lane p). No detectable PCR amplification was found in the RT reactions with parental RKO or RKO-pBABE (vector alone) RNA after priming with oligonucleotide 1 (Fig. 1C, lanes d to g; data not shown for PCR primer pairs 4 and 1 and 4 and 3). These results demonstrate that these clones express either FB2F or ENA/FB2F *ATM* fragments and that the expression of pBABE-*ATM* fragments can be selectively distinguished from endogenous *ATM* expression (expression data not shown for RKO FB2F clone 9). No amplification was detectable in RT-PCRs lacking reverse transcriptase, demonstrating the absence of DNA contamination in the total RNA preparations (Fig. 1C, lanes c, j, m, and o). Due to the lack of ATM antibodies which specifically recognize protein fragments corresponding to the ENA and FB2F regions of ATM, protein expression of these fragments could not be determined. Western blots of full-length ATM protein revealed no significant changes in endogenous ATM protein levels in any of these clones (data not shown).

ATM-LZ fragment expression causes RDS. Cell lines derived from AT patients normally exhibit a defect in S-phase arrest known as RDS in response to IR (26, 43). The effects of FB2F and ENA/FB2F fragment expression on S-phase arrest following IR in RKO cells were assessed as the initial test of whether LZ expression affects ATM function. Inhibition of DNA synthesis is manifested as a decrease in thymidine incorporation in irradiated cells relative to unirradiated cells at early time points after IR. Following exposure to 4 Gy of IR, the parental RKO cells and control transfectant exhibited an approximately 50% decrease in DNA synthesis. In contrast, the AT fibroblast cell line GM5849 exhibited a lack of inhibition of DNA synthesis in response to IR (Fig. 2). Similar to the AT GM5849 cell line, RKO-LZ clones FB2F3, -9, and -12 and ENA/FB2F18 exhibited AT-like RDS (Fig. 2; data not shown for clone 9). These results indicate that S-phase arrest in response to IR can be abrogated in a tumor cell line expressing these LZ motif-containing ATM fragments.

ATM-LZ fragment expression decreases cell survival and enhances chromosomal aberrations after IR. Radiation sensitivity of ATM FB2F and ENA/FB2F fragment-expressing clones was assessed by a clonogenic survival assay. Consistent with previously published reports of hypersensitivity of AT cells to IR, the GM5849 AT fibroblast cell line was significantly more sensitive to IR than the parental RKO or control transfectant (Fig. 3). However, the ATM-LZ-expressing RKO clones, FB2F12 and ENA/FB2F18, were sensitive to IR, with survival rates comparable to that of the AT cell line. The RKO clone FB2F3 exhibited an intermediate sensitivity to IR (Fig. 3). These data demonstrate that expression of the ATM FB2F or ENA/FB2F fragments in RKO cells can lead to enhanced radiosensitivity, characteristic of cells derived from AT patients.

ATM-LZ clones, along with isogenic and nonisogenic controls, were synchronized in G_1 and then treated with gamma rays to determine induction of chromosomal breaks in G_1 and residual damage at metaphase. Chromosome aberrations in G_1 phase were analyzed by using the premature chromosome condensation technique (46). An increase in chromosomal breaks in G_1 phase is apparent with an increasing dose of IR (Fig. 4A). The number of chromosomal breaks per cell in RKO clones FB2F3 (data not shown), FB2F12, and ENA/FB2F18 at 2 and 4 Gy of IR were greater than the number of aberrations in control cells and were similar to those seen in the AT

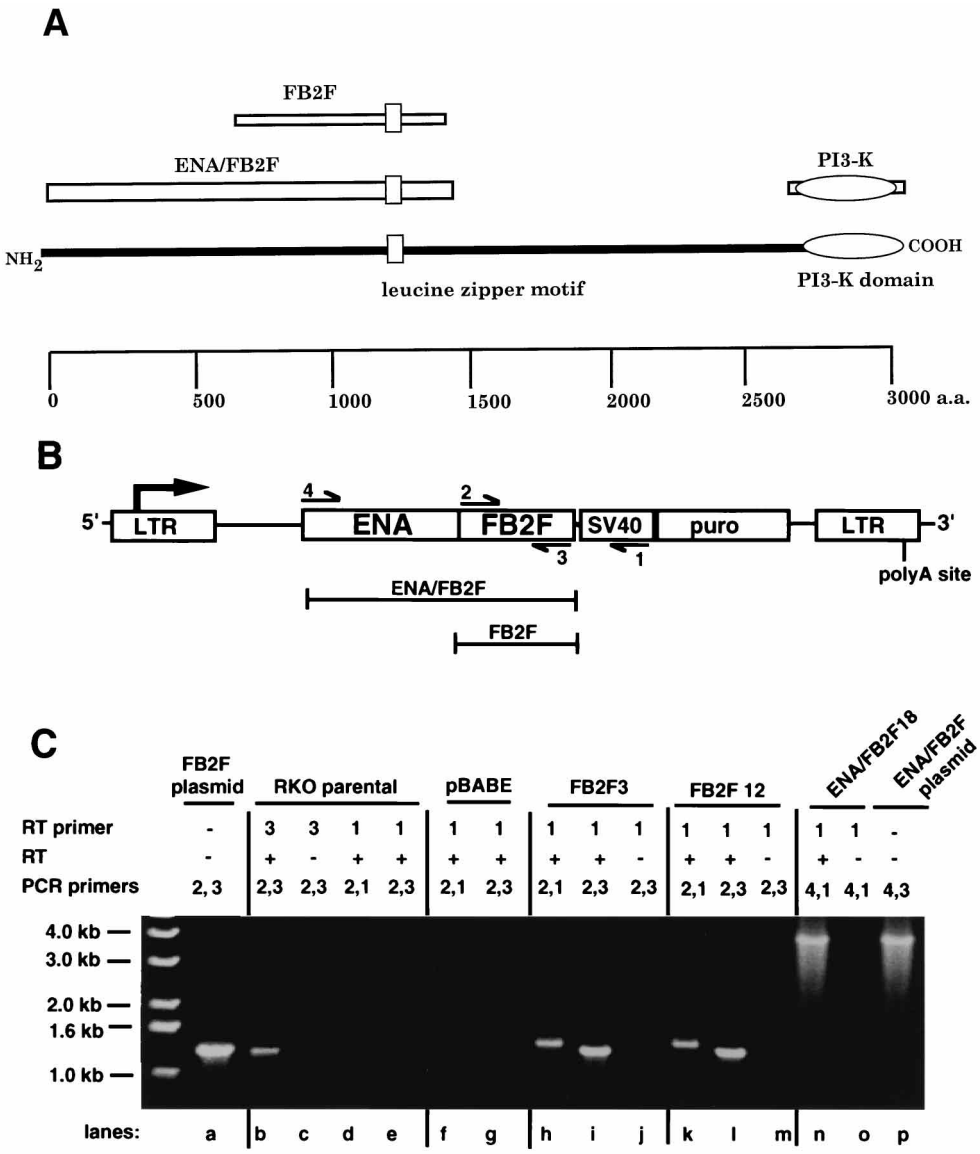

FIG. 1. Expression of the ATM LZ fragments in a RKO colorectal tumor cell line. (A) Diagram of *ATM* cDNA fragments encoding segments of the full-length ATM protein. The ATM protein is denoted as a thick black line representing approximately 3,000 amino acids (a.a.). The LZ and PI3-kinase domains are represented by a rectangle and an oval, respectively. All clones were drawn to approximate scale. (B) Diagram of the pBABE retroviral vector subcloned with either the FB2F or ENA/FB2F cDNA fragments. Oligonucleotides used for RT-PCR analysis are shown as primers 1 to 4. (C) RT-PCR analysis of RKO clones infected with pBABE-FB2F or -ENAFB2F retroviruses. Either primer 1 or 3 was used for RT in the absence or presence of Superscript RT. Primer pairs 2 and 3, 2 and 1, 4 and 1, or 4 and 3 were used for cDNA amplification as indicated. The PCR products were electrophoresed on an ethidium bromide-stained agarose gel.

homozygote-derived cell line (GM5849). To determine the residual damage, cells were allowed to repair the damage and then allowed to go to metaphase. When chromosome aberrations were analyzed at metaphase 24 h after irradiation, RKO FB2F12 cells, in particular, revealed significantly higher levels ($P < 0.001$, Student's t test) of chromosomal damage (including both chromatid and chromosome types of aberrations), exhibiting an approximately fourfold increase in total chromosomal aberrations at 2 and 4 Gy of IR (Fig. 4B). Interestingly, all of the ATM dominant-negative clones showed statistically higher levels ($P < 0.05$) of chromatid type of damage at both 2 and 4 Gy, suggesting the presence of a repair defect. The ATM-LZ-expressing RKO cells did not appear to be as defective as cells from AT patients, since the GM5849 SV40-transformed AT fibroblasts exhibited an even greater number of chromosomal aberrations than the FB2F12 clone following IR treatment in this assay (data not shown).

To examine chromosomal aberrations induced in the G_2/M phase of the cell cycle, metaphase chromosome spreads were isolated at early time points following 1 Gy of IR and examined for chromosomal gaps and breaks. An increased number of chromosomal gaps and breaks per metaphase was noted for all cell lines within 30 min following IR treatment compared to the unirradiated cells (Fig. 4C). At all time points following IR, however, the number of gaps and breaks per metaphase of RKO FB2F and ENA/FB2F clones was significantly higher than the RKO parental cell line. The number of gaps and breaks per metaphase of the RKO clones FB2F12 and FB2F9 changed little between 30 and 150 min following IR treatment, whereas the number of gaps and breaks per metaphase of the

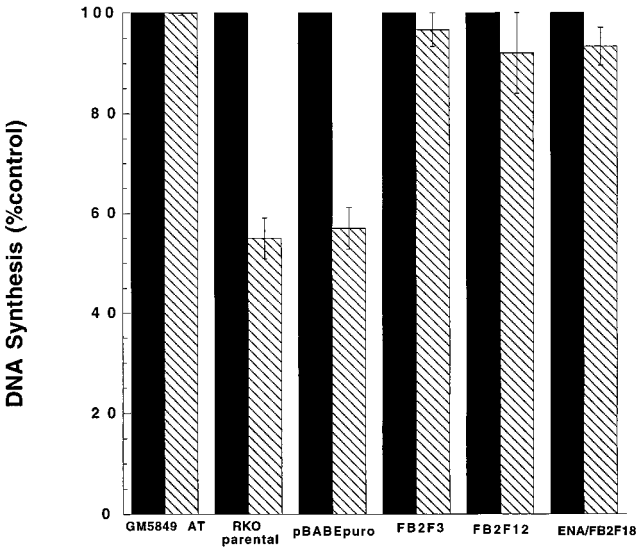

FIG. 2. ATM LZ fragment expression causes RDS. AT cells (GM5849), RKO parental cells, or RKO clones expressing either vector alone, FB2F, or ENAFB2F fragments were assessed for DNA synthesis 30 min following treatment with 0 (solid bars) or 4 (hatched bars) Gy of IR. S-phase arrest is manifest as a decrease in thymidine incorporation in irradiated cells relative to unirradiated cells. Experiments were performed in triplicate; error bars represent SE.

parental RKO cell line steadily decreased over time following IR treatment. The number of aberrations in the cells expressing the ATM-LZ fragments approached that seen in fibroblasts from AT patients by this assay (see Fig. 9 below).

Effects of ATM-LZ fragment expression on p53-induction and G_1 and G_2 arrests. In addition to the S-phase checkpoint defect (RDS) in AT cells, G_1 and G_2 checkpoint defects have been reported. Cells derived from AT patients exhibit defective and/or delayed increases in p53 protein and in p53-dependent gene products such as the G_1 cdk inhibitor, p21, following IR (6). To determine whether RKO cells expressing FB2F or ENA/FB2F fragments also fail to induce the p53-dependent pathway, levels of p53 and p21 protein were assessed by immunoblotting. Increased levels of p53 and p21 protein in response to IR were apparent in the normal GM2184 lymphoblastoid cell line and parental RKO cells, whereas minimal levels of p53 and p21 induction were evident in the AT cell line GM1526 (Fig. 5). RKO clones expressing either FB2F or ENA/FB2F fragments exhibited an increase in both p53 and p21 protein levels in response to IR comparable to the control cell lines. In addition to normal p53 and p21 induction responses, these same clones also exhibited an arrest in the G_1 phase of the cell cycle following IR treatment as assessed by flow cytometric analysis (data not shown). Therefore, in contrast to a loss of the p53-independent S-phase cell cycle arrest induced by IR (Fig. 2), these results suggest that expression of ATM-LZ fragments in RKO cells does not appear to significantly abrogate the IR-induced, p53-dependent signal transduction pathway that leads to a G_1 arrest.

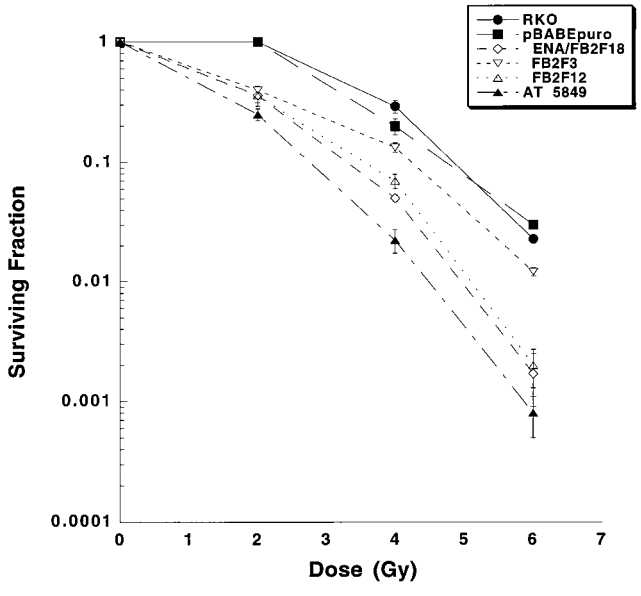

FIG. 3. Expression of ATM LZ fragments enhances radiosensitivity. AT cells, parental RKO cells, and RKO clones were exposed to 0, 2, 4, and 6 Gy of IR and then incubated for 8 days prior to fixation, staining, and assessment of colony formation. Clonogenic survival assays were performed in triplicate; mean colony numbers relative to unirradiated colony numbers are plotted, and the SE are shown as error bars.

RKO cells expressing FB2F or ENA/FB2F fragments were also assessed for G_2 checkpoint abnormalities in response to IR. Normally, there is a decrease in the number of cells entering mitosis 30 to 90 min after IR treatment, thus decreasing the mitotic index. In contrast, AT cells irradiated in the G_2 phase of the cell cycle will continue to enter into mitosis at these early time points following irradiation. The G_2/M checkpoint was thus determined by evaluating the number of mitotic indices at various time points after IR. Parental RKO cells and RKO-LZ-expressing cells exhibited similar decreases in the number of cells entering mitosis after IR. At 150 min following 1 Gy of IR, the mitotic index decreased from a mean of 19 mitoses per 1,000 cells to a mean of 2 mitoses per 1,000 cells in all of these RKO cells and clones examined. Thus, the RKO-LZ-expressing cells were not significantly different than the parental cells in their ability to arrest in G_2 after IR.

Expression of the PI3K ATM fragment in AT cells. The functional role of the ATM PI3K domain (Fig. 1A) was assessed by expressing the PI3K homology sequence in AT cells and determining whether expression of this fragment functionally complements the phenotypic defects of AT cells. Neomycin-resistant, normal (GM637) or AT (GM5849) SV40-transformed fibroblast clones, infected with either recombinant LXSN or LXSN-PI3K retroviruses, were isolated and screened for the expression of the PI3K cDNA fragment by RT-PCR. To differentiate between the expression of endogenous *ATM* and recombinant LXSN-PI3K *ATM* fragments in the 637 clonal populations, an oligonucleotide primer was used in the RT reaction which is complementary only to the LXSN-SV40 sequence (Fig. 6A, primer 1). To detect endogenous *ATM* expression in the GM637 normal cell line, an oligonucleotide primer was used in a RT reaction which is complementary to the transcribed strand of the *ATM* PI3K RNA sequence (Fig. 6A, primer 3). RT-PCR of 637 PI3K clone 1 and 5849 PI3K clones 4 and 10 resulted in the selective amplification of an approximately 1.3-kb or 1.2-kb cDNA product (Fig. 6B, lanes h, i, k, l, n, and o). The size of the 1.2-kb product was in agreement with the amplified PI3K plasmid DNA and the amplified endogenous *ATM* PI3K cDNA (Fig. 6B, lanes a and b, respectively). No endogenous *ATM* PI3K cDNA was detectable in parental GM5849 cells when primer 3 was used in the RT reaction (data not shown). No PCR amplification was detectable when primer 1 was used in the RT reaction of parental GM637 or 5849-LXSN RNA (vector alone) (Fig. 6B,

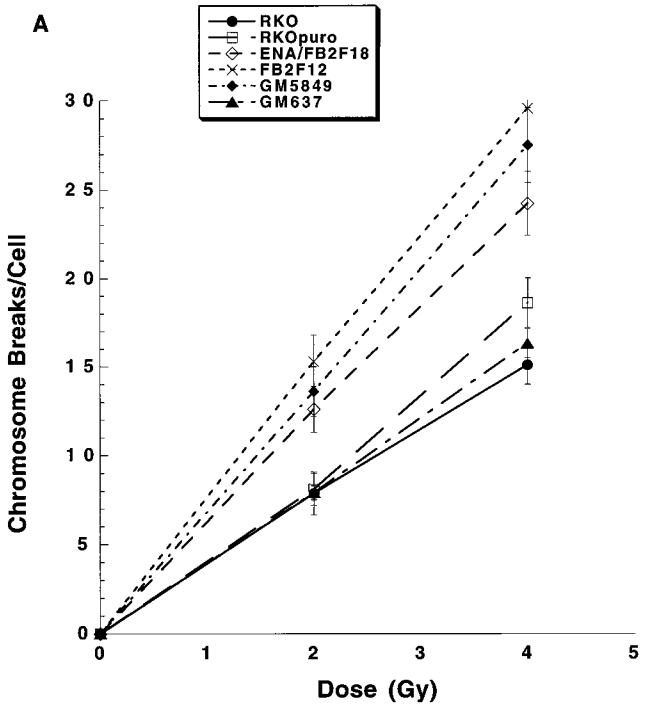

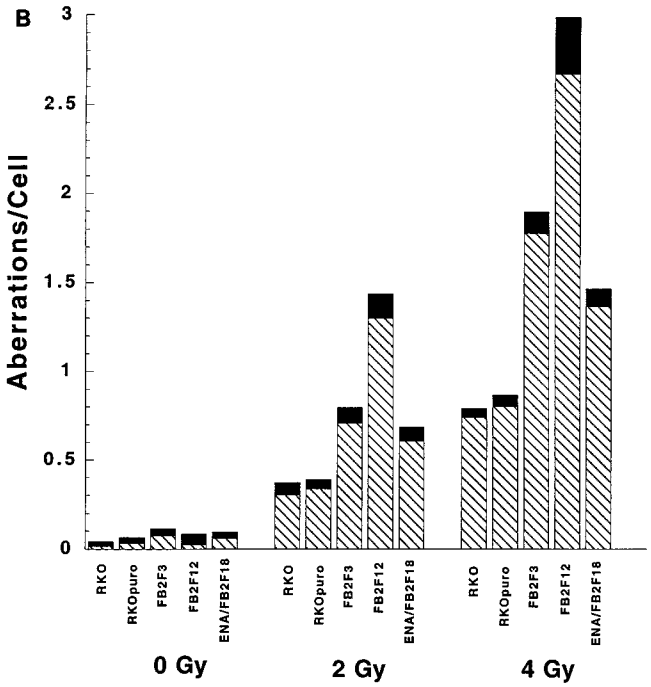

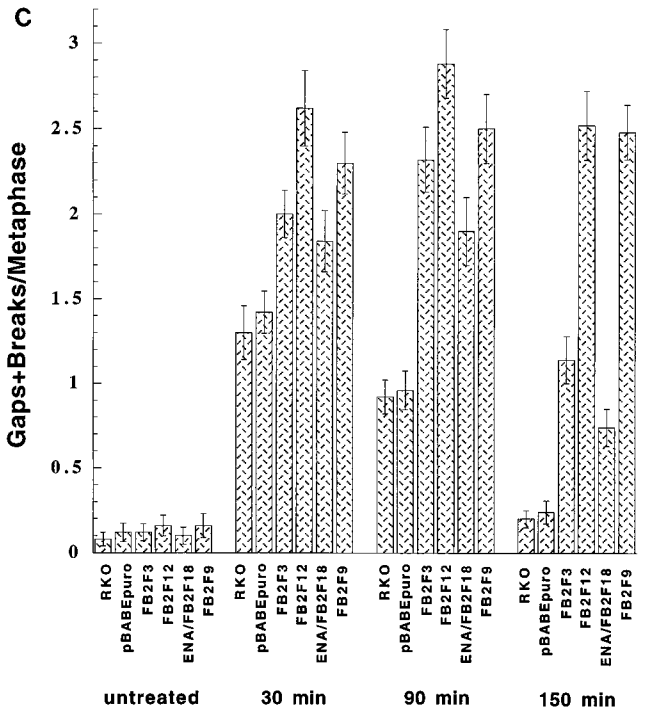

FIG. 4. Expression of ATM LZ fragments enhances IR-induced chromosomal aberrations. (A) Initial levels of chromosome damage as a function of dose in G_1-phase cells as determined by premature chromosome condensation technique. Chromosome damage is expressed as the extra number of chromosome fragments per cell determined by subtracting the number of chromosome fragments per cell in the unirradiated cells from that found in the irradiated cells. The means of 25 cells are plotted and the SE between two independent experiments are shown as error bars. (B) These same synchronized clones were analyzed for residual damage at metaphase 24 h after irradiation. Chromosomal aberrations are represented as chromatid type (breaks, gaps, or exchanges) (solid bars) or chromosome type (deletions and dicentric and centric rings) (hatched bars). (C) Metaphase chromosome spreads were prepared from parental RKO cells and RKO clones harvested in log-phase growth with no irradiation (untreated) or harvested at 30, 90, or 150 min following 1 Gy of ionizing radiation and examined for chromosomal breaks and gaps.

lanes d to g). These results demonstrate that 637 and 5849 clones express LXSN-PI3K fragments (expression data not shown for 5849 PI3K clone 2). No amplification was detectable in RT-PCRs lacking reverse transcriptase (Fig. 6B, lanes c, j, m, and p).

PI3K ATM fragment expression restores irradiation-induced S-phase arrest. PI3K fragments were assessed for their ability to complement RDS in an AT fibroblast cell line. The parental GM637 and 637 PI3K1 normal cell lines exhibited an approximately 50% decrease in DNA synthesis after irradiation. In contrast, the AT fibroblast cell lines GM5849 and 5849-LXSNneo failed to inhibit DNA synthesis in response to IR (Fig. 7). Similar to the normal GM637 cell line, however, AT 5849 PI3K clones exhibited an approximately 45 to 50% decrease in DNA synthesis after IR (Fig. 7). These results demonstrate restoration of the S-phase arrest in response to IR in these AT cells.

ATM PI3K fragment expression rescues radiosensitivity and chromosomal breakage. A clonogenic survival assay was performed to determine whether PI3K fragment expression in an AT cell line can rescue the radiation sensitivity phenotype. The clonal AT cell line, 5849 PI3K10, no longer showed radiation sensitivity as the survival curves were comparable to the normal GM637 and 637 PI3K1 cell lines (Fig. 8). The 5849 PI3K4 clone exhibited an intermediate restoration of radiosensitivity (data not shown). These data demonstrate that expression of the PI3K domain in an AT cell line leads to enhanced clonogenic survival after irradiation.

To determine whether the expression of PI3K fragments in an AT cell line rescues IR-induced chromosomal abnormalities, the number of chromosomal aberrations in 637 and 5849 clones expressing the PI3K domain was assessed in the G_2 phase of the cell cycle. An increasing number of chromosomal gaps and breaks per metaphase was noted for all cell lines within 30 min following IR treatment compared to the un-

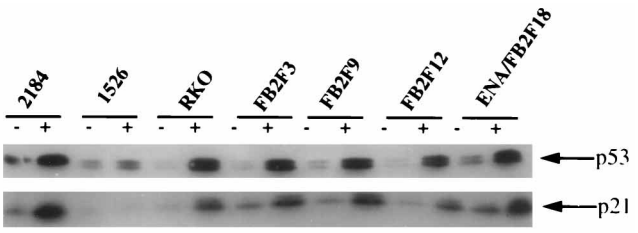

FIG. 5. Expression of ATM LZ fragments does not abrogate IR-induced p53 or p21 induction. Normal (GM2184) or AT (GM1526) lymphoblasts, control RKO cells, and RKO cells expressing LZ fragments were irradiated at 0 (−) or 4 (+) Gy and harvested for immunoblot analysis for either p53 or p21 3 h following IR.

treated cells (Fig. 9). The number of gaps and breaks per metaphase of the parental AT GM5849 and 5849-LXSNneo cells, assessed at 30, 90, and 150 min after IR treatment, was significantly higher than those of the normal GM637 and 637 PI3K-expressing cells. The AT 5849 cells expressing the PI3K fragment exhibited a significant decrease in the number of gaps and breaks per metaphase at 90 and 150 min relative to the control 5849 cell lines. However, these clones still contained a higher number of chromosomal aberrations than the normal GM637 cell line. These data demonstrate that while expression of the ATM PI3K fragment in AT cells results in fewer irradiation-induced gaps and breaks than the parental GM5849 AT cell line, the PI3K domain only partially complements IR-induced chromosomal breakage in these cells. Complementation of the G_1 and G_2 checkpoints could not be adequately evaluated because these checkpoints are abnormal even in the control cells due to the SV40 transformation.

DISCUSSION

A human tumor cell line expressing ATM LZ-containing fragments has been created which largely recapitulates the AT phenotype. These sequences serve as dominant-negative fragments in a human tumor cell line as revealed by RDS, decreased clonogenic survival, and enhanced chromosomal aberrations following gamma irradiation. The creation of dominant-negative fragments of ATM provides a mechanism by which many of the functions of ATM can be inhibited in any transfectable cell type and thus provides an advantage over the use of restricted AT cell types, such as EBV-immortalized lymphoblasts or SV40-transformed fibroblasts, for physiological studies. In addition, the creation of a variety of cell types with defective ATM function will enable investigation of cell-type-specific effects of ATM function in many cellular processes, such as cell cycle control, radiosensitivity, or growth factor responses. For example, a cell line of neural crest origin with defective ATM function could be used to evaluate the role of ATM in neurotrophin signalling pathways. AT patients exhibit particular sensitivity to cell death in cerebellar Purkinje cells, but it has been difficult to clearly demonstrate whether this cell death is due to abnormal responses to oxidative stress or to abnormal responses to growth factor signalling pathways (cell death induced by limiting cytokine amounts). Now that other cell types with dysfunctional ATM can be created, one can better evaluate the role ATM may play in radiation-induced apoptosis versus apoptosis caused by limiting growth factor signalling.

While the expression of ATM-LZ fragments in a human tumor cell line enhanced radiosensitivity and chromosomal breakage, and abrogated the S-phase checkpoint following IR treatment, these same fragments did not block p53 induction or the G_1 or G_2 checkpoints in response to DNA damage. Abrogation of some ATM-dependent functions, but not others, has the advantage of allowing the study of distinct cellular pathways and the roles that certain proteins may play in one cellular process versus another. Generation of human tumor cell lines containing intact p53 function, but exhibiting radiosensitivity and lack of DNA-damage-inducible S-phase arrest, suggests that these deficits are not dependent on disruption of

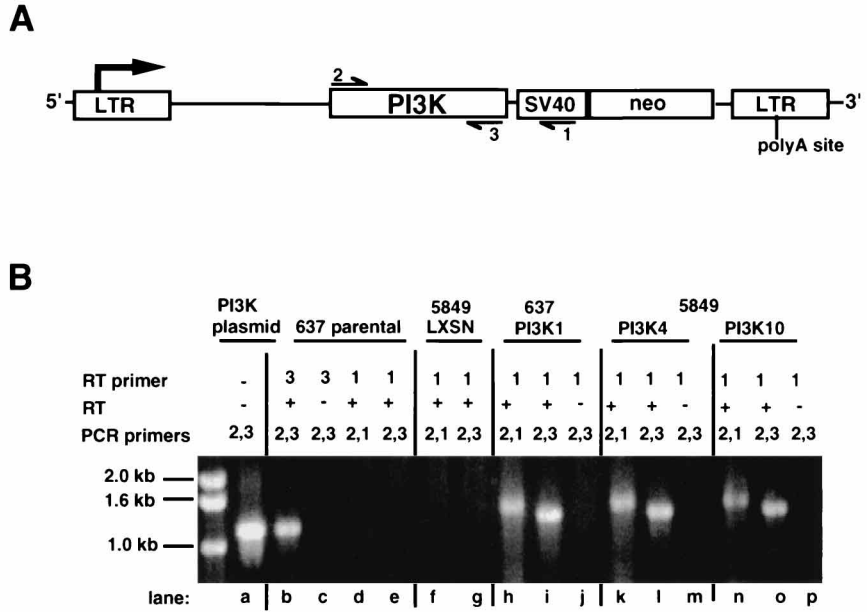

FIG. 6. Expression of the ATM PI3-kinase fragment in AT cells. (A) Diagram of the LXSN retroviral vector subcloned with the *ATM* PI3K cDNA fragment. Oligonucleotides used for RT-PCR analysis are shown as primers 1 to 3. (B) RT-PCR analysis of parental cells and normal (637) and AT (5849) clones infected with LXSN alone or LXSN-PI3K retroviruses. cDNA synthesis was performed using primer 1 or 3 in the absence or presence of Superscript RT. Primer pairs 2 and 3 or 2 and 1 were used for cDNA amplification. The PCR products were electrophoresed on an ethidium bromide-stained agarose gel.

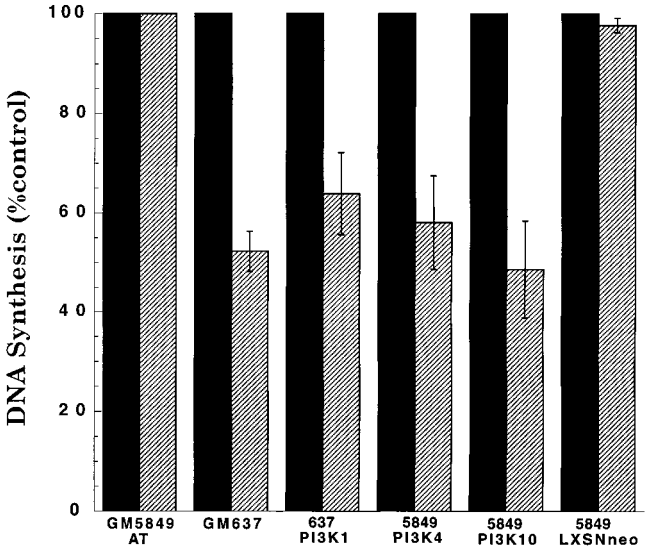

FIG. 7. Expression of PI3K fragment restores IR-induced S-phase arrest in AT cells. Control cells and normal (637) and AT (5849) SV40-transformed fibroblasts expressing the PI3K fragment were measured for RDS following treatment with 0 (solid bars) or 4 (hatched bars) Gy of IR as described in the legend for Fig. 2. Experiments were performed in triplicate; error bars represent SE.

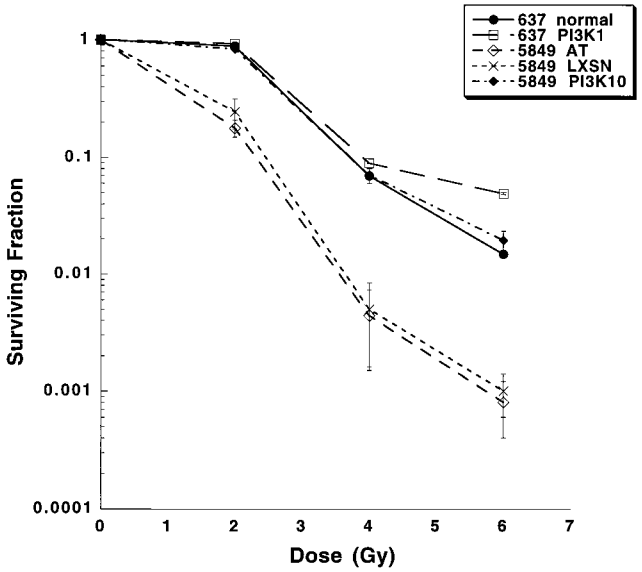

FIG. 8. Expression of ATM PI3K fragment in AT cells reduces radiosensitivity. Parental and control cells and AT (5849) and normal (637) clones expressing the PI3K domain were exposed to 0, 2, 4, and 6 Gy of IR and then incubated for 2 weeks prior to fixation, staining, and assessment of colony formation. Clonogenic survival assays were performed in triplicate; SE are shown as error bars.

the p53 pathway. It has previously been reported that a DNA-damage-inducible S-phase arrest is independent of p53 status (33); however, the role that p53 plays in radiosensitivity in AT is not entirely clear. In order to more definitively assess the role of p53 in ATM-modulated radiosensitivity, the effects of ATM dysfunction in p53 null cells are currently being investigated.

The observation that expression of ATM-LZ fragments enhances chromosomal instability, but does not significantly alter the ability of these cells to arrest in G_1 or G_2 after IR, suggests that defective G_1 or G_2 checkpoints in AT cells are not responsible for the enhanced IR-induced chromosomal breakage and radiosensitivity in AT cells. Since the IR-induced G_2 checkpoint was not complete in these RKO cells and small numbers of mitotic cells from both parental and ATM-LZ clones could be evaluated after irradiation, chromosomal aberrations could still be assessed. Since there was no significant alteration in the G_2 arrest capabilities in these cell types, the increased chromosomal breakage in the RKO-LZ clones must be attributable to some other factor, such as problems with DNA lesion processing or DNA repair. The S-phase checkpoint defect could not be responsible for this difference since clones which never entered S-phase exhibited increased chromosomal breakage (Fig. 4A) and since increased chromosomal breakage was evident in cells which were already in G_2 at the time of irradiation (early time points) (Fig. 4C). Interestingly, recent studies in yeasts have suggested that abnormalities in the processing of DNA lesions could contribute to cell cycle checkpoint abnormalities and/or radiosensitivity (35).

While expression of ATM LZ-containing fragments creates an "AT-like" phenotype in the RKO cells, it remains to be demonstrated whether these fragments affect cellular function in an ATM-dependent manner. These fragments were initially chosen for ATM manipulation studies due to the homology of a core sequence within the *ATM* cDNA to a LZ motif. Although it is unknown whether this motif can be expressed as a true LZ fragment, one could hypothesize that these fragments form dimers with ATM or heterodimers with other protein targets integral to ATM function, thereby resulting in a dominant-negative inhibition of ATM activity. Studies are in progress assessing in vitro and in vivo protein-protein interactions among LZ-containing ATM fragments, ATM, and other proteins implicated in the ATM-dependent signal transduction pathways.

Expression of the ATM PI3K domain in AT SV40-transformed fibroblasts resulted in the functional complementation of some phenotypic AT defects, including restoration of IR-induced S-phase arrest, radiosensitivity, and partial reduction of chromosomal instability. The observation that no endogenous *ATM* mRNA or truncated protein in the AT GM5849 cell line was detectable by RT-PCR or Western blot analysis (data not shown) argues against the possibility of intragenic complementation as the mechanism by which the PI3K domain is complementing phenotypic defects of AT. Complementation of p53 induction and G_1 arrest in response to IR in AT cells expressing the PI3K fragment could not be assessed due to the fact that these fibroblasts are T-antigen-expressing SV40-transformed cells. In addition, consistent with the results of Paules et al. (48), we found an abnormal G_2 checkpoint in these SV40-transformed cells; thus, complementation of the G_2 checkpoint defect in AT could not be assessed in the transfected clones. To circumvent these problems, it will be useful to introduce the PI3K fragment into AT cells with intact G_1 and G_2 checkpoints, such as EBV-immortalized AT lymphoblasts or primary fibroblasts.

Complementation of RDS, radiosensitivity, and reduction in chromosomal instability by AT cells expressing the PI3K fragment suggests that this PI3K domain of ATM (and possibly of ATM homologs) is critical for function. Although it has not yet been determined whether the PI3K domain in ATM exhibits lipid or protein kinase activity, some ATM homologs shown to have protein kinase activity include the catalytic subunit of DNA-PK (21) and the yeast proteins Tel1p and Mec1P (52,

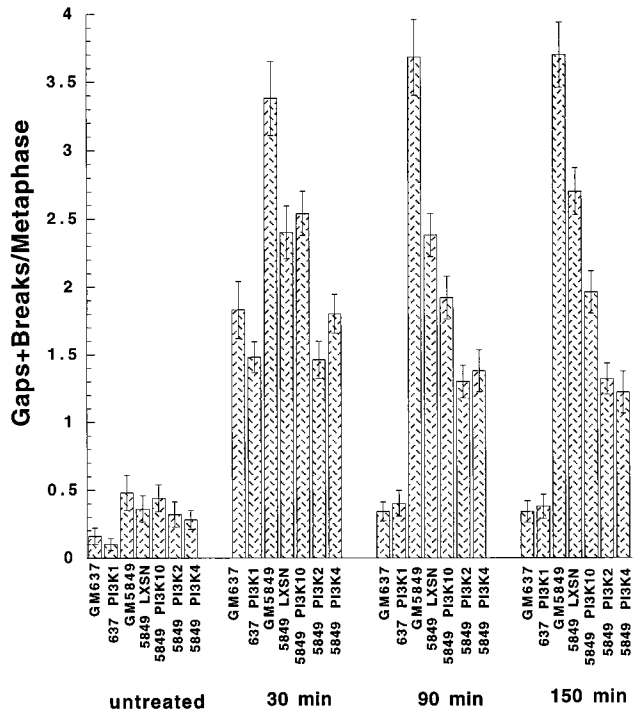

FIG. 9. Expression of PI3K domain reduced chromosomal breakage in AT cells. Metaphase chromosome spreads derived from parental, control, and PI3K-expressing normal (637) and AT (5849) clones were isolated at 30, 90, or 150 min following 1 Gy of ionizing radiation and examined for chromosomal gaps and breaks. Error bars indicate SE.

57). Tel1p and Mec1p were recently found to phosphorylate a downstream target, Rad53p, one of several proteins necessary for regulating the rate of progression through S phase in response to DNA damage. It is possible that the mechanism by which ATM PI3K fragment expression restores S-phase arrest in AT cells occurs through interaction of the PI3K domain with downstream human Rad53 homologs.

The rescue of radiosensitivity in AT SV40-transformed fibroblasts by expression of the PI3K domain may be due in part to PI-3 kinases serving as "survival factors." Indeed, PI-3 kinase was shown to be required for the inhibition of apoptotic cell death in a rat pheochromocytoma cell line by nerve growth factor (64). The hypersensitivity of AT cells to IR and radiomimetic drugs could be due to a defective response to growth factor-induced signalling pathways requiring ATM kinase activity. Although previous studies suggest that other foreign cDNAs can also rescue the radiosensitivity of AT cells (7, 38, 65), our observations that the ATM PI3K domain complements not only radiosensitivity but also RDS and IR-induced chromosomal breakage support the conclusion that this domain may be specifically serving an important function of ATM. To more accurately determine the role of the PI-3 kinase domain in our complementation studies, however, we are in the process of expressing mutant PI-3 kinase domains in AT cells and assessing the effects of these mutated domains in cell cycle control, radiosensitivity, and chromosomal instability.

Though functional complementation of many of the AT defects appears to be occurring with expression of the PI3K domain alone, this does not suggest that the remainder of this large protein is unimportant for ATM function. In fact, the dominant-negative effects of the ATM-LZ fragments suggest that ATM interacts with itself or other proteins for optimal function. However, since this small PI-3 kinase domain enhances survival and reduces RDS in AT cells, it could be a potentially useful reagent for complementation of the ATM defect in AT patients.

In summary, two functional domains of ATM which provide new insights into its mechanism of action have been identified. The ability to manipulate ATM activity in cell lines provides a means by which specific pathways using ATM can be better characterized and understood. Targeting essential domains within the *ATM* gene, such as the PI3K and LZ domains, could potentially be exploited to render cells more susceptible to IR and certain radiomimetic chemicals. Observed increases in radiosensitivity at a clinically relevant dose of 2 Gy makes targeting of ATM function particularly attractive for therapeutic enhancement.

ACKNOWLEDGMENTS

We thank George Thomas and Carol Miller for help with mitotic cell preparation and assays, Alan Friedman for generously providing the retroviral expression vectors, and Christine Canman and Janet Siliciano for helpful discussions.

This work was supported in part by grants from the AT Children's Project and the National Institutes of Health (CA71387, ES05777, and NS34746). M.B.K. is the Steven Birnbaum Scholar of the Leukemia Society of America.

REFERENCES

1. **Al-Khodairy, F., E. Fotou, K. S. Sheldrick, D. J. F. Griffiths, A. R. Lehmann, and A. M. Carr.** 1994. Identification and characterization of new elements involved in checkpoint and feedback controls in fission yeast. Mol. Biol. Cell **5:**147–160.
2. **Allen, J. B., Z. Zhou, W. Siede, E. C. Friedberg, and S. J. Elledge.** 1994. The SAD1/RAD53 protein kinase controls multiple checkpoints and DNA damage-induced transcription in yeast. Genes Dev. **8:**2401–2415.
3. **Beamish, H., K. K. Khanna, and M. F. Lavin.** 1994. Ionizing radiation and cell cycle progression in ataxia telangiectasia. Radiat. Res. **138:**S130–S133.
4. **Brown, E. J., M. W. Albers, T. B. Shin, K. Ichikawa, C. T. Keith, W. S. Lane, and S. L. Schreiber.** 1994. A mammalian protein targeted by G1-arresting rapamycin-receptor complex. Nature **369:**756–758.
5. **Byrd, P. J., C. M. McConville, P. Cooper, J. Parkhill, T. Stankovic, G. M. McGuire, J. A. Thick, and A. M. R. Taylor.** 1996. Mutations revealed by sequencing the 5-prime half of the gene for ataxia-telangiectasia. Hum. Mol. Genet. **5:**145–149.
6. **Canman, C. E., A. C. Wolff, C. Chen, A. J. Fornace, and M. B. Kastan.** 1994. The p53-dependent G1 cell cycle checkpoint pathway and ataxia-telangiectasia. Cancer Res. **54:**5054–5058.
7. **Chen, P., A. A. Girjes, K. Hobson, H. Beamish, K. K. Khanna, A. Farrell, M. Gatei, B. Teale, M. Buchwald, R. Legerski, and M. F. Lavin.** 1996. Genetic complementation of radiation response by 3′ untranslated regions (UTR) of RNA. Int. J. Radiat. Biol. **69:**385–395.
8. **Dang, C. V., M. McGuire, M. Buckmire, and W. M. F. Lee.** 1989. Involvement of the "leucine zipper" region in the oligomerization and transforming activity of human c-myc protein. Nature **337:**664–666.
9. **Dhand, R., I. Hiles, G. Panayotou, S. Roche, M. J. Fry, I. Gout, N. F. Totty, O. Truong, P. Vicendo, K. Yonezawa, M. Kasuga, S. A. Courtneidge, and M. D. Waterfield.** 1994. PI 3-kinase is a dual specificity enzyme: autoregulation by an intrinsic protein-serine kinase activity. EMBO J. **13:**522–533.
10. **Enoch, T., and C. Norbury.** 1995. Cellular responses to DNA damage: cell-cycle checkpoints, apoptosis and the roles of p53 and ATM. Trends Biochem. Sci. **20:**426–430.
11. **Freund, G. G., J. G. Wittig, and R. A. Mooney.** 1995. The PI3-kinase serine kinase phosphorylates its p85 subunit and IRS-1 in PI3-kinase/IRS-1 complexes. Biochem. Biophys. Res. Commun. **206:**272–278.
12. **Gatti, R. A., E. Boder, H. V. Vinters, R. S. Sparkes, A. Norman, and K. Lange.** 1991. Ataxia-telangeictasia: an interdisciplinary approach to pathogenesis. Medicine **70:**99–117.
13. **Gibbas, L. M., and L. G. Jackson.** 1985. A new hypotonic solution for cytogenetic analysis of leukemic bone marrow cells. Karyogram **11:**91–92.
14. **Gilad, S., R. Khosravi, D. Shkedy, T. Uziel, Y. Ziv, K. Savitsky, G. Rotman, S. Smith, L. Chessa, T. J. Jorgensen, R. Harnik, M. Frydman, O. Sanal, S. Portnoi, Z. Goldwicz, N. G. J. Jaspers, R. A. Gatti, G. Lenoir, M. F. Lavin, K. Tatsumi, R. D. Wegner, Y. Shiloh, and A. Bar-Shira.** 1996. Predominance of null mutations in ataxia-telangiectasia. Hum. Mol. Genet. **5:**433–439.
15. **Gottlieb, T. M., and S. P. Jackson.** 1993. The DNA-dependent protein kinase: requirement for DNA ends and association with Ku antigen. Cell **72:**131–142.
16. **Granger-Schnarr, M., E. Benusiglio, M. Schnarr, and P. Sassone-Corsi.**

1992. Transformation and transactivation suppressor activity of the c-Jun leucine zipper fused to a bacterial repressor. Proc. Natl. Acad. Sci. USA **89:**4236–4239.
17. **Greenwell, P. W., S. L. Krommal, S. E. Porter, J. Gassenhuber, B. Obermaier, and T. D. Petes.** 1995. Tel1, a gene involved in controlling telomere length in S. cerevisiae, is homologous to the human ataxia telangiectasia gene. Cell **82:**823–829.
18. **Hanks, S. K., A. M. Quinn, and T. Hunter.** 1988. The protein kinase family: conserved features and deduced phylogeny of the catalytic domains. Science **241:**42–52.
19. **Hari, K. L., A. Santerre, J. J. Sekelsky, K. S. McKim, J. B. Boyd, and R. S. Hawley.** 1995. The *mei-41* gene of *D. melanogaster* is a structural and functional homolog of the human ataxia telangiectasia gene. Cell **82:**815–821.
20. **Harnden, D. G.** 1994. The nature of ataxia-telangiectasia: problems and perspectives. Int. J. Radiat. Biol. **66:**S13–19.
21. **Hartley, K. O., D. Gell, G. C. M. Smith, H. Zhang, N. Divecha, M. A. Connelly, A. Admon, S. P. Lees-Miller, C. W. Anderson, and S. P. Jackson.** 1995. DNA-dependent protein kinase catalytic subunit—a relative of phosphatidylinositol 3-kinase and the ataxia telangiectasia gene product. Cell **82:**849–856.
22. **Hecht, F., and B. K. Hecht.** 1990. Cancer in ataxia-telangiectasia patients. Cancer Genet. Cytogenet. **46:**9–19.
23. **Heitman, J., N. R. Movva, and M. N. Hall.** 1991. Targets for cell cycle arrest by the immunosuppressant rapamycin in yeast. Science **253:**905–909.
24. **Helliwell, S. B., P. Wagner, J. Kunz, M. Deuter-Reinhard, R. Henriquez, and M. N. Hall.** 1994. TOR1 and TOR2 are structurally and functionally similar but not identical phosphatidylinositol kinase homologues in yeast. Mol. Biol. Cell **5:**105–118.
25. **Hiles, I. D., M. Otsu, S. Volinia, M. J. Fry, I. Gout, R. Dhand, G. Panayotou, F. Ruiz-Larrea, A. Thompson, H. F. Totty, J. J. Hsuan, S. A. Courtneidge, P. J. Parker, and M. Waterfield.** 1992. Phosphatidylinositol 3-kinase: structure and expression of the 110 kd catalytic subunit. Cell **70:**419–429.
26. **Houldsworth, J., and M. F. Lavin.** 1980. Effect of ionizing radiation on DNA synthesis in ataxia-telangiectasia cells. Nucleic Acids Res. **8:**3709–3720.
27. **Kastan, M. B., Q. Zhan, W. S. El-Deiry, F. Carrier, T. Jacks, W. V. Walsh, B. S. Plunkett, B. Vogelstein, and A. J. Fornace Jr.** 1992. A mammalian cell cycle checkpoint pathway utilizing p53 and GADD45 is defective in ataxia-telangiectasia. Cell **71:**587–597.
28. **Kato, J., M. Matsuoka, D. K. Strom, and C. J. Sherr.** 1994. Regulation of cyclin D-dependent kinase 4 (cdk4) by cdk4-activating kinase. Mol. Cell. Biol. **14:**2713–2721.
29. **Khanna, K. K., and M. F. Lavin.** 1993. Ionizing radiation and UV induction of p53 protein by different pathways in ataxia-telangiectasia cells. Oncogene **8:**3307–3312.
30. **Kobayashi, Y., B. Tycko, A. L. Soreng, and J. Sklar.** 1991. Transrearrangements between antigen receptor genes in normal human lymphoid tissues and in ataxia telangiectasia. J. Immunol. **147:**3201–3209.
31. **Kuerbitz, S. J., B. S. Plunkett, W. V. Walsh, and M. B. Kastan.** 1992. Wild-type p53 is a cell cycle checkpoint determinant following irradiation. Proc. Natl. Acad. Sci. USA **89:**7491–7495.
32. **Kunz, J., R. Henriquez, U. Schneider, M. Deuter-Reinhard, N. R. Movva, and M. N. Hall.** 1993. Target of rapamycin in yeast, TOR2, is an essential phosphatidylinositol kinase homolog required for G1 progression. Cell **73:**585–596.
33. **Larner, J. M., H. Lee, and J. L. Hamlin.** 1994. Radiation effects on DNA synthesis in a defined chromosomal replicon. Mol. Cell. Biol. **14:**1901–1908.
34. **Lipkowitz, S., M. H. Stern, and I. R. Kirsh.** 1990. Hybrid T cell receptor genes formed by interlocus recombination in normal and ataxia-telangiectasia lymphocytes. J. Exp. Med. **172:**409–418.
35. **Lydall, D., and T. Weinert.** 1995. Yeast checkpoint genes in DNA damage processing: implications for repair and arrest. Science **270:**1488–1491.
36. **McKinnon, P. J.** 1987. Ataxia-telangiectasia: an inherited disorder of ionizing-radiation sensitivity in man. Progress in the elucidation of the underlying biochemical defect. Hum. Genet. **75:**197–208.
37. **Meyn, M. S.** 1993. High spontaneous intrachromosomal recombination rates in ataxia-telangiectasia. Science **260:**1327–1330.
38. **Meyn, M. S., J. M. Lu-Kuo, and L. B. Herring.** 1993. Expression cloning of multiple human cDNAs that complement the phenotypic defects of ataxia-telangiectasia group D fibroblasts. Am. J. Hum. Genet. **53:**1206–1216.
39. **Miller, A. D., D. G. Miller, J. G. Victor, and C. M. Lynch.** 1993. Use of retroviral vectors for gene transfer and expression. Methods Enzymol. **217:**581–599.
40. **Morgenstern, J. P., and H. Land.** 1990. Advanced mammalian gene transfer: high titre retroviral vectors with multiple drug selection markers and a complementary helper-free packaging cell line. Nucleic Acids Res. **18:**3587–3596.
41. **Morrow, D. M., D. A. Tagle, Y. Shiloh, F. S. Collins, and P. Hieter.** 1995. *TEL1*, an *S. cerevisiae* homolog of the human gene mutated in ataxia telangiectasia, is functionally related to the yeast checkpoint gene *MEC1*. Cell **82:**831–840.
42. **Nagasawa, H., S. A. Latt, M. E. Lalande, and J. B. Little.** 1985. Effects of X-irradiation on cell-cycle progression, induction of chromosomal aberrations and cell killing in ataxia-telangiectasia (AT) fibroblasts. Mutat. Res. **148:**71–82.
43. **Painter, R. B., and B. R. Young.** 1980. Radiosensitivity in ataxia-telangiectasia: a new explanation. Proc. Natl. Acad. Sci. USA **77:**7315–7317.
44. **Pandita, T. K., S. Pathak, and C. R. Geard.** 1995. Chromosome end associations, telomeres and telomerase activity in ataxia telangiectasia cells. Cytogenet. Cell Genet. **71:**86–93.
45. **Pandita, T. K., and C. R. Geard.** 1996. Chromosome aberrations in human fibroblasts induced by monoenergetic neutrons. 1. Relative biological effectiveness. Radiat. Res. **145:**730–739.
46. **Pandita, T. K., E. J. Hall, T. K. Hei, M. A. Piatyszek, W. E. Wright, C. Q. Piao, R. K. Pandita, J. C. Willey, R. C. Geard, M. B. Kastan, and J. W. Shay.** 1996. Chromosome end-to-end associations and telomerase activity during cancer progression in human cells after treatment with alpha-particles stimulating radon progeny. Oncogene **13:**1423–1430.
47. **Pandita, T. K., and W. N. Hittelman.** 1992. The contribution of DNA and chromosome repair deficiencies to the radiosensitivity of ataxia-telangiectasia. Radiat. Res. **131:**214–223.
48. **Paules, R. S., E. N. Levedakou, S. J. Wilson, C. L. Innes, N. Rhodes, T. D. Tlsty, D. A. Galloway, L. A. Donehower, M. A. Tainsky, and W. K. Kaufmann.** 1995. Defective G2 checkpoint function in cells from individuals with familial cancer syndromes. Cancer Res. **55:**1763–1773.
49. **Sabatini, D. M., H. Erdjument-Bromage, M. Lui, P. Tempst, and S. H. Snyder.** 1994. RAFT1: a mammalian protein that binds to FKBP12 in a rapamycin-dependent fashion and is homologous to yeast TORs. Cell **78:**35–43.
50. **Sabers, C. J., M. M. Martin, G. J. Brunn, J. M. Williams, F. J. Dumont, G. Wiederrecht, and R. T. Abraham.** 1995. Isolation of a protein target of the FKBP12-rapamycin complex in mammalian cells. J. Biol. Chem. **270:**815–822.
51. **Sambrook, J., E. F. Fritsch, and T. Maniatis.** 1989. Molecular cloning: a laboratory manual. Cold Spring Harbor Laboratory Press, Cold Spring Harbor, N.Y.
52. **Sanchez, Y., B. A. Desany, W. J. Jones, Q. Liu, B. Wang, and S. J. Elledge.** 1996. Regulation of Rad53 by the ATM-like kinases Mec1 and Tel1 in yeast cell cycle checkpoint pathways. Science **271:**357–360.
53. **Savitsky, K., A. Bar-Shira, S. Gilad, G. Rotman, Y. Ziv, L. Vanagaite, D. A. Tagle, S. Smith, T. Uziel, S. Sfez, M. Ashkenazi, I. Pecker, M. Frydman, R. Harnik, S. R. Patanjali, A. Simmons, G. A. Clines, A. Sartiel, R. A. Gatti, L. Chessa, O. Sanal, M. F. Lavin, N. G. J. Jaspers, A. M. R. Taylor, C. F. Arlett, T. Miki, S. M. Weissman, M. Lovett, F. S. Collins, and Y. Shiloh.** 1995. A single ataxia telangiectasia gene with a product similar to PI-3 kinase. Science **268:**1749–1753.
54. **Savitsky, K., S. Sfez, D. A. Tagle, A. Sartiel, F. S. Collins, Y. Shiloh, and G. Rotman.** 1995. The complete sequence of the coding region of the ATM gene reveals similarity to cell cycle regulators in different species. Hum. Mol. Genet. **4:**2025–2032.
55. **Shiloh, Y.** 1995. Ataxia-telangiectasia: closer to unraveling the mystery. Eur. J. Hum. Genet. **3:**116–138.
56. **Stan, R., M. M. McLaughlin, R. Cafferkey, R. K. Johnson, M. Rosenberg, and G. P. Livi.** 1994. Interaction between FKBP12-rapamycin and TOR involves a conserved serine residue. J. Biol. Chem. **269:**32027–32030.
57. **Sun, Z., D. S. Fay, F. Marini, M. Foiani, and D. F. Stern.** 1996. Spk1/Rad53 is regulated by Mec1-dependent protein phosphorylation in DNA replication and damage checkpoint pathways. Genes Dev. **10:**395–406.
58. **Swift, M., D. Morrell, R. B. Massey, and C. L. Chase.** 1991. Incidence of cancer in 161 families affected by ataxia-telangiectasia. N. Engl. J. Med. **325:**1831–1836.
59. **Swift, M., P. J. Reitnauer, D. Morrell, and C. L. Chase.** 1987. Breast and other cancers in families affected by ataxia-telangeictasia. N. Engl. J. Med. **316:**1289–1294.
60. **Taccioli, G. E., T. M. Gottlieb, T. Blunt, A. Priestley, J. Demengeot, R. Mizuta, A. R. Lehmann, F. W. Alt, S. P. Jackson, and P. A. Jeggo.** 1994. Ku80: product of the XRCC5 gene and its role in DNA repair and V(D)J recombination. Science **265:**1442–1445.
61. **Tanti, J. F., T. Gremeaux, E. Van Obberghen, and Y. LeMarchand-Brustel.** 1994. Insulin receptor substrate 1 is phosphorylated by the serine kinase activity of phosphatidylinositol 3-kinase. Biochem. J. **304:**17–21.
62. **Tuteja, N., M. Meyer, K. K. Reddy, J. R. Falck, R. Aneja, A. Parra, D. J. Burns, L. M. Ballas, and L. C. Cantley.** 1994. Human DNA helicase II: a novel DNA unwinding enzyme identified as the Ku autoantigen. J. Biol. Chem. **269:**32358–32367.
63. **Weinert, T. A., G. L. Kiser, and L. H. Hartwell.** 1994. Mitotic checkpoint genes in budding yeast and the dependence of mitosis on DNA replication and repair. Genes Dev. **8:**652–665.
64. **Yao, K.-S., M. Clayton, and P. J. O'Dwyer.** 1995. Apoptosis in human adenocarcinoma HT29 cells induced by exposure to hypoxia. J. Natl. Cancer Inst. **87:**117–122.
65. **Ziv, Y., A. Bar-Shira, T. J. Jorgensen, P. S. Russell, A. Sartiel, T. B. Shows, R. L. Eddy, M. Buchwald, R. Legerski, R. T. Schimke, et al.** 1995. Human cDNA clones that modify radiomimetic sensitivity of ataxia-telangiectasia (group A) cells. Somatic Cell Mol. Genet. **21:**99–111.